Design, XRD/HSA-interactions, spectral, thermal, Solvatochromism and DNA-binding of two [Cu(phen)(triene)]Br2 complexes: Experimental and DFT/TD-DFT investigations

Article *in* Journal of Molecular Structure · January 2021

DOI: 10.1016/j.molstruc.2021.129983

CITATION
1

READS
106

9 authors, including:

Firas Awwadi
University of Jordan
107 PUBLICATIONS **1,442** CITATIONS
SEE PROFILE

Salim F. Haddad
University of Jordan
187 PUBLICATIONS **1,147** CITATIONS
SEE PROFILE

Nabil Al-Zaqri
King Saud University
63 PUBLICATIONS **206** CITATIONS
SEE PROFILE

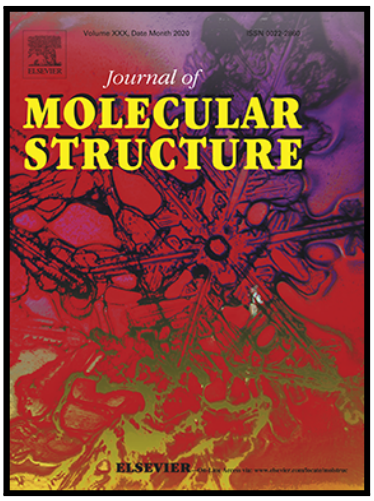

Design, XRD/HSA-interactions, spectral, thermal, Solvatochromism and DNA-binding of two [Cu(phen)(triene)]Br_2 complexes: Experimental and DFT/TD-DFT investigations

Muheeb Fuqha , Firas F. Awwadi , Salim F. Haddad , Nabil Al-Zaqri , Fahad A. Alharthi , Mohammed Suleiman , Abdelkader Zarrouk , Ahmed M. Boshaala , Ismail Warad

PII: S0022-2860(21)00114-9
DOI: https://doi.org/10.1016/j.molstruc.2021.129983
Reference: MOLSTR 129983

To appear in: *Journal of Molecular Structure*

Received date: 4 September 2020
Revised date: 15 January 2021
Accepted date: 17 January 2021

Please cite this article as: Muheeb Fuqha , Firas F. Awwadi , Salim F. Haddad , Nabil Al-Zaqri , Fahad A. Alharthi , Mohammed Suleiman , Abdelkader Zarrouk , Ahmed M. Boshaala , Ismail Warad , Design, XRD/HSA-interactions, spectral, thermal, Solvatochromism and DNA-binding of two [Cu(phen)(triene)]Br_2 complexes: Experimental and DFT/TD-DFT investigations, *Journal of Molecular Structure* (2021), doi: https://doi.org/10.1016/j.molstruc.2021.129983

Highlights

- Two new complexes of type [Cu(phen)(triene)]Br_2 were prepared in excellent yields.
- DFT, TGA, XRD and spectral analysis were used for the characterization.
- The DNA-binding affinities of both complexes were evaluated.
- TD-DFT and electron transfer for both complexes were modeled.

Design, XRD/HSA-interactions, spectral, thermal, Solvatochromism and DNA-binding of two [Cu(phen)(triene)]Br_2 complexes: Experimental and DFT/TD-DFT investigations

Muheeb Fuqha[1], Firas F. Awwadi[2], Salim F. Haddad[2], Nabil Al-Zaqri[3], Fahad A. Alharthi[3], Mohammed Suleiman[1], Abdelkader Zarrouk[4], Ahmed M. Boshaala[5], Ismail Warad[6,*]

[1]Department of Chemistry, Science College, An-Najah National University, P.O. Box 7, Nablus, Palestine
[2]Chemistry Department, Faculty of Science, The University of Jordan, Amman 11942, Jordan
[3]Department of Chemistry, College of Science, King Saud University, P.O. Box 2455, Riyadh 11451, Saudi Arabia
[4]Laboratory of Materials, Nanotechnology and Environment, Faculty of Sciences, Mohammed V University, Av. Ibn Battouta, Box 1014, Agdal-Rabat, Morocco
[5]Department of Chemistry, Faculty of Science, Benghazi University, P O Box 1308 Benghazi, Libya
[6]Department of Chemistry and Earth Sciences, College of Arts and Sciences, Qatar University, P.O. Box 2713, Doha, Qatar

ismail.warad@najah.edu

Abstract

Two dicationic Cu(II) complexes of [Cu(phen)(NNN)]Br_2 (**1-2**) general formula [phen = 1,10-phenanthroline, NNN = diethelenetriamine (dien) (**1**) and dipropylenetriamine (dipn)(**2**)], have been synthesized in very good yields. The two complexes were characterized *via* UV-vis., CHN-EA, MS, FT-IR, thermal, and X-ray crystallographic techniques. XRD data for **1** showed a distorted square pyramidal Cu(II) ions geometry center with three uncoordinated water molecules. TGA were performed to evaluate the interactions strength and found to support the XRD molecular interactions results. The time-dependent density functional theory (TD-DFT) and electron transfer processes were modeled, and consequently the absorption maxima around 610 and 280 nm were attributed to d–d and Phen(π)→Phen(π^*) transitions. Positive Gutmann's solvatochromism behavior of both complexes have been recorded. Furthermore, the ability of the two complexes for DNA binding was evaluated *via* absorption studies in the visible region showing high K_b constant values.

Keywords: Cu(II); Phen; NNN-tridentate; XRD; solvatochromism, DNA.

1. Introduction

The synthesis of 1,10-phenanthroline/metal ion complexes received extensive attention in research due to their significant applications [1, 2] as potential anti-tumor agents [3, 4]. Those mixed-ligand complexes containing nitrogen donor ligands have also great potential in antimicrobial [1-4], antioxidant [5], anticancer, and catalytic activities [6-9]. The photo-physical properties of Cu(II) complexes including polypyridine ligands resulted in effective DNA binder complexes [10-15]. The anticancer effectiveness Cu(II) complexes are categorized according to their ability to inhibit DNA binding [16]. The determination of the complex structures in solid-state and solutions is vital to understand the intelligent biological processes in biological systems [17, 18]. For instance, copper(II) complexes with phenanthroline chelating agent possess hydrophilic groups that allow them to act as promising anti-tumor agents due to their cell membrane penetration ability [19-20].

Diethelenetriamine (dien) and dipropylenetriamine (dipn) are N-tridentate chelate ligands which can form bi five-membered N-M rings. Moreover, N-tridentate chelate ligands usually form dinuclear, trinuclear and metal clusters [21]. Recently, we have inspected similar [Cu(N-N)(dipn)]Br_2 and [Cu(bipy)dipn)].$2BF_4$ complexes in spectral and biological activities [22-28]. In this work, our group is reporting the mixed-ligands combination of two new dicationic Cu(phen)(NNN)]Br_2 complexes [NNN = diethelenetriamine (dien) (**1**) and dipropylenetriamine (dipn) (**2**)]. The complexes structural properties were spectral and the thermally monitored, moreover, the crystal structure of **1** was solved, the electron transfer was modeled by TD-DFT, and their ability for DNA binding was evaluated.

2. Methods

2.1. Chemicals

All chemicals and solvents used were purchased from Sigma–Aldrich.

*2.2. General procedure to synthesis of [Cu(phen)(NNN]Br_2 (**1-2**)*

(0.81 g, 2 mmol) of $Br_2Cu(phen)$ was suspended in 30 mL of ethanol under ultrasound waves, 2 mmol of diethylenetriamine or dipropylenetriamine in 10 mL of water and then were merged to the previous solution. The reaction was stirred under ultrasound for 8 min. until the color was turned to deep blue color. The solvents were evaporated from the solution under vacuum and the solid product was washed well using CH_2Cl_2 solvent then dried under vacuum. Suitable XRD crystals of **1** have been collected via slow evaporation of water from **1** stock solution.

*2.2.2. [Cu(phen)(dien)]Br_2 (**1**)*

Yield (87 mg, 85%), m.p. = 180 °C. MS m/z 505.2 {[Cu(phen)(dien)]Br_2} [M^+] for $C_{16}H_{21}Br_2CuN_5$ Calculated: C, 37.92; H, 4.18; N, 13.82. Found C, 37.81; H, 4.10; N, 14.62%, IR (KBr, νcm^{-1}): 3460(ν_{H2O}), 3380 and 3280, (ν_{H-N}), 3120 (ν_{C-H} of phenyl), 2800-2950 (ν_{C-H}), 1580 (ν_{N-H}), 1160 (ν_{N-C}), 620 and 540 (ν_{Cu-N}). UV–Vis in water: λ_{max} (ε_{max}/ $M^{-1}cm^{-1}$): 282 (1.6×10^3), 610 (3.5×10^2).

*2.2.3. [Cu(phen)(dipn)]Br_2 (**2**)*

Yield (96 mg, 90%), M.p. = 190 °C. MS m/z 533.2 [M^+] for $C_{18}H_{25}Br_2CuN_5$ Calculated: C, 40.43; H, 4.71; N, 13.10. Found C, 40.22; H, 4.64; N, 13.08%, IR (KBr, νcm^{-1}): 3440 (ν_{H2O}), 3360 and 3270, (ν_{H-N}), 3160 (ν_{C-H} of phenyl), 2940 (ν_{C-H}), 1560 (ν_{N-H}), 1180 (ν_{N-C}), 610 and 520 (ν_{Cu-N}).UV–Vis in water: λ_{max} (ε_{max}/ $M^{-1}cm^{-1}$): 280 (1.4×10^3), 610 (3.0×10^2).

2.3. Physical analysis

CHN-microanalyses were done on an Elementar Varrio EL analyzer. TGA were performed at TA instrument SDT-Q600 in air. The FT-IR spectra were obtained using Perkin–Elmer 621 spectrophotometer. UV-Vis. spectra were determined on Pharmacia LKB-Biochrom 4060 spectrophotometer. The melting points were recorded using Stuart® SMP10. The MS were performed using ThermoScientific™ TSQ Altis™ Triple Quadrupole Mass Spectrometer.

2.4. XRD-collection and computational details

Full geometry optimization of **1** was carried out using DFT at the B3LYP level [29]. All computations were performed using the GAUSSIAN09 package [30]. For C, H and N the cc-pvdz basis set were assigned, while for Cu the LanL2DZ basis set with effective core potential were employed [31]. Vertical electronic excitations based on B3LYP optimized geometries were computed using the TD-DFT formalism in water using polarizable continuum model (PCM) [32-36].

A suitable block like elongated green crystal of **1** was mounted with Epoxy on a glass fiber and the diffraction data were collected at room temperature using an Oxford Xcalibur diffractometer (Mo Kα radiation, λ = 0.7107 Å). Data was reduced and processed to give *hkl* files using CrysAlisPro software [37]. The structures were solved by direct methods and refined by least-squares method on F2 using the SHELXTL program package [38]. Carbon bound hydrogen atoms were placed in calculated positions and refined isotropically using a riding model, whereas, the six hydrogen atoms of the three water of salvation were located in a difference Fourier map and were refined isotropic ally. All non-hydrogen atoms were refined anisotropically. Highest peak and deepest hole are 0.949 and -0.503 e/ Å3. Details of crystal data collection and refinement are given in Table 1.

Table 1. Structure refinement and crystal data of **1.**

Complex No.	Complex **1**
CCDC	982731
Formula weight	740.99 ($C_{16}H_{21}Br_2CuN_5$.Phen.$3H_2O$)
Temperature	293(2) K
Wavelength	0.71073 Å
Crystal system	Monoclinic
Space group	*P* $2_1/n$
Unit cell dimensions	*a* = 12.6411(13) Å, *b* = 19.422(3) Å, β= 111.016(12)°, *c* = 13.7128(13) Å
Volume	3142.7(6) $Å^3$
Z	4
Density (calculated)	1.566 Mg/m^3
Absorption coefficient	3.279 mm^{-1}
F(000)	1500
Crystal size	0.4687 x 0.2661 x 0.2059 mm^3
Theta range for data collection	3.18 to 26.00°
Index ranges	$-15 \leq h \leq 15$, $-23 \leq k \leq 14$, $-15 \leq l \leq 16$
Reflections collected	13451
Independent reflections	6161 [R(int) = 0.0344]
Completeness to theta = 27.50°	99.8 %
Absorption correction	Analytical
Max. and min. transmission	0.652 and 0.395
Goodness-of-fit on F^2	1.013
Final R indices [I>2sigma(I)]	R1 = 0.0602, wR2 = 0.1408
R indices (all data)	R1 = 0.1130, wR2 = 0.1612

2.5. DNA binding experiment.

The DNA binding tests were performed in pH 7.4, Tris-HCl buffer using distilled water as solvent. The DNA titration processes with the complexes were in the visible regions at 610 nm for **1** and at 610 nm for **2** using fixed complexes concentration $5x10^{-3}$M and different DNA concentration 0–0.04M [22-28].

3. Result and Discussion

3.1. Synthesis

[Cu(phen)(NNN)]Br_2 **(1-2)** as dicationic Cu(II) complexes have been prepared using mixed-ligands, phen = 1,10-phenanthroline, NNN= diethelenetriamine (dien) (**1**) and dipropylenetriamine (dipn) (**2**)]. Reacting of [Cu(Phen)Br_2] starting complex with NNN ligands under ultrasonic revealed the formation of the desired complexes as bromide salts with high yields (Scheme 1). The complexes found to be highly stable in open atmosphere solid state, high boiling points were recorded, moreover, these complexes are good water soluble with blue color in both solid and aqua-states. The complexes were characterized using MS, CHN-EA and spectral methods (see experimental part). The XRD- structure of **1** reflected the formation of the Cu(II) center with distorted square pyramidal shape.

3.1. Synthesis

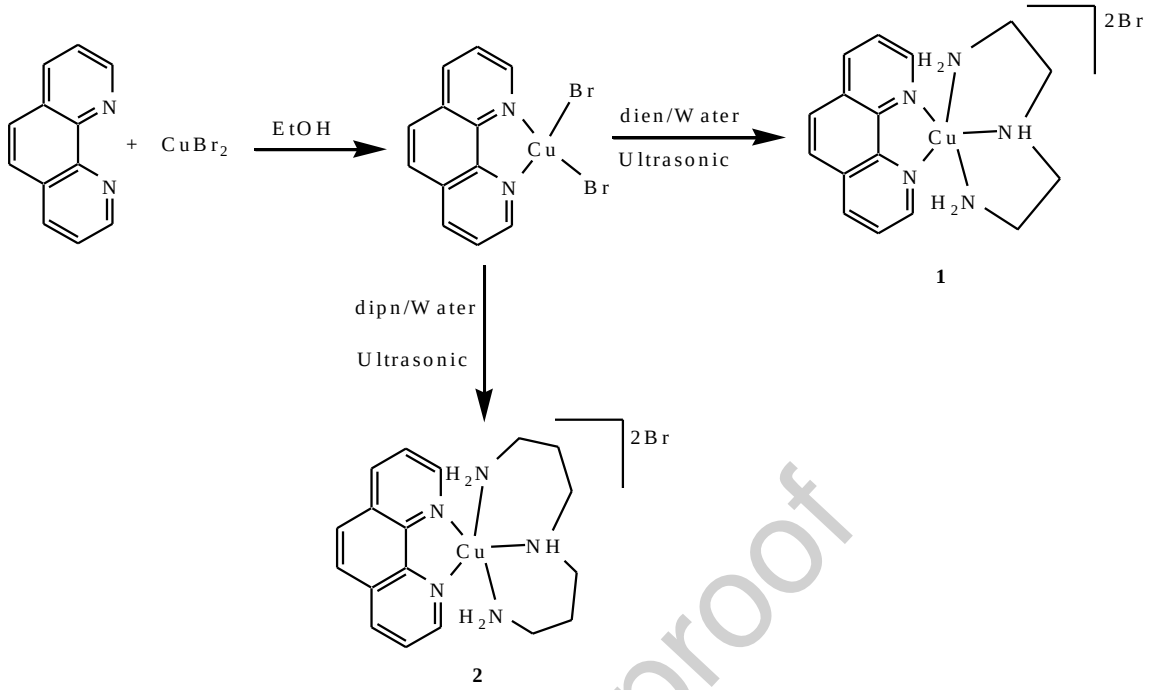

Scheme-1: Synthesis of [Cu(phen)(NNN)]Br_2 **(1-2)**

3.2. IR

The KBr-IR disk spectra of $CuBr_2$(phen) starting complex was compared to **1** and **2** after triamines addition as seen in Fig. 1. It was observed that only in **1** and **2** the stretching vibrations at 3460 $\nu_{(O\text{-}H)}$ and 1430 $\nu_{(bend)}$ corresponded to H_2O since water has been detected in the lattice of the complexes. In the spectra of the **1** and **2** (not in $CuBr_2$(phen) complex), the three stretching vibrations at 3400-3320, 3280–3200 and 1620-1590 cm^{-1} assigned to $\nu s_{N–H}$, $\nu_{asN–H}$ and $\delta_{N–H}$, respectively shifted to lower wavenumbers compared to their free triamines ligands. This observation strongly confirm that amine groups coordinated to the Cu(II) center [39]. The stretching vibrations at 3120-3050 cm^{-1} is due to C-H phenylic stretching vibration, meanwhile, C-H of sp^3 hybridization alkyl stretching vibrations were sited at 2800-2950 cm^{-1} [40-47]. Peak

at ~ 620 and 540 cm^{-1} can be attributed to $\nu_{(Cu-N)}$ new bond formation [44]. A stretching vibrations at 282-295 cm^{-1} can be cited to the $\nu_{(Cu-Br)}$ bonds [45].

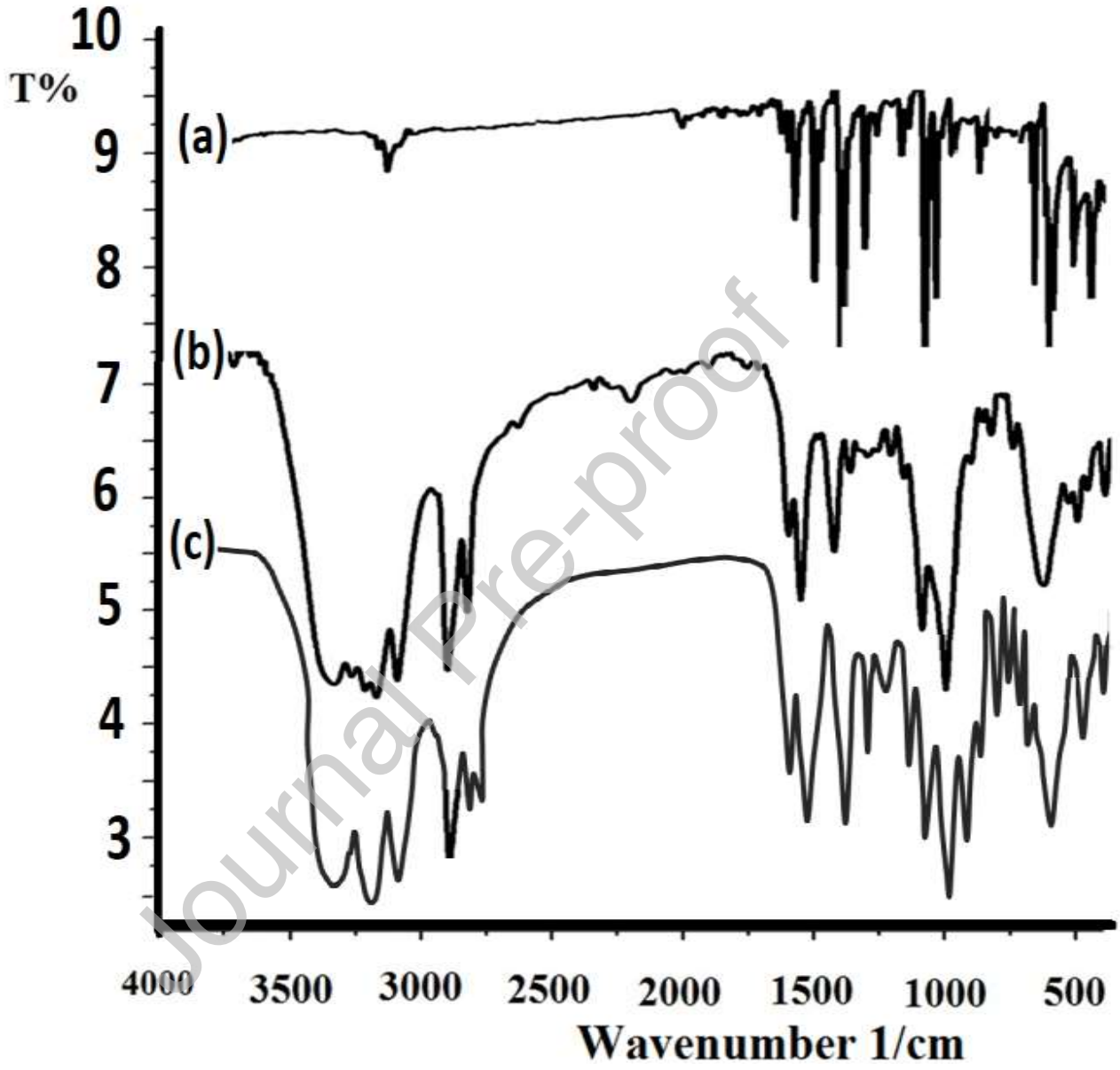

Fig. 1. FT-IR of (a) $CuBr_2$(phen), (b) **1,** and (c) **2**.

*3.3. Crystal structure of **1***

1 crystallized in the Monoclinic with $P2_1/n$ space group. Elected experimental and DFT computed bond distances and angles of **1** and **2** are given in Table 2. The asymmetric unit with atomic numbering scheme is shown in Fig. 2.

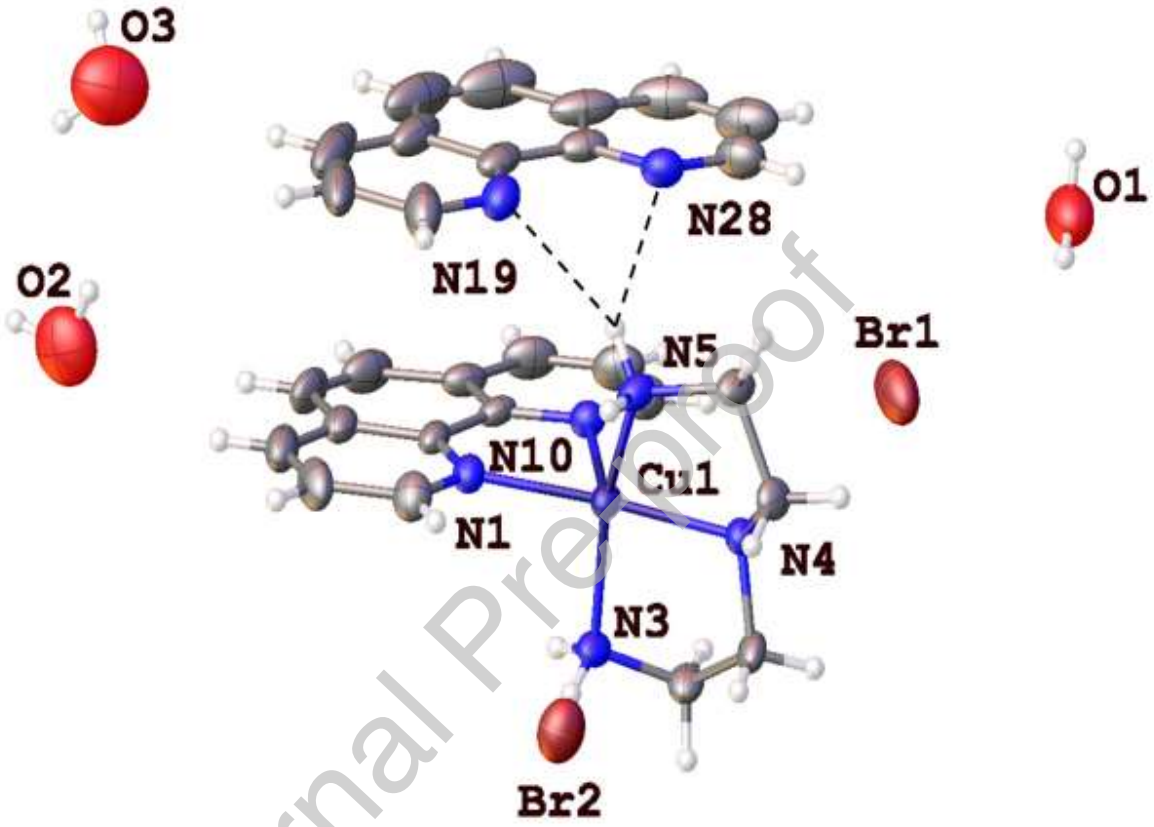

Fig. 2. The ORTEP generated diagram of **1** with 50% probability displacement ellipsoids.

Table 2. XRD/DFT selected bond lengths [Å] and angles [°] for **1** and **2**.

No.	Bond lengths	Exp./XRD of **1** [Å]	DFT of **1** [Å]	DFT of **2** [Å]
1	Cu(1)-N(10)	2.212 (4)	2.267	2.301
2	Cu(1)-N(3)	2.036 (3)	2.088	2.085
3	Cu(1)-N(1)	2.030 (4)	2.066	2.071
4	Cu(1)-N(4)	2.020(3)	2.075	2.101
5	Cu(1)-N(5)	2.015 (4)	2.088	2.120

No.	Angles	Exp./XRD of **1** [°]	DFT of **1** [°]	DFT of **2** [°]
1	N(5)-Cu(1)-N(1)	95.66 (15)	95.34	96.43
2	N(4)-Cu(1)-N(1)	175.14 (16)	171.98	172.89
3	N(5)-Cu(1)-N(3)	155.91 (15)	155.81	155.61
4	N(4)-Cu(1)-N(3)	84.17 (14)	83.16	83.46
5	N(1)-Cu(1)-N(3)	94.00 (15)	95.39	95.43
6	N(5)-Cu(1)-N(10)	109.66 (14)	101.84	108.94
7	N(4)-Cu(1)-N(10)	105.80 (16)	109.78	107.88
8	N(1)-Cu(1)-N(10)	78.85 (16)	78.23	78.73
9	N(3)-Cu(1)-N(10)	93.83 (14)	101.54	101.84
10	N(5)-Cu(1)-N(4)	84.17 (14)	83.19	84.02

As shown in the Table 2, high degrees of similarities in the angles and bonds lengths of the two complexes were collected when compared the XRD-experimental with the DFT-theoretical calculations. For complex **1**, the Cu^{2+} ion is coordinated by two N-atoms of the phen and three N-atoms of triene ligands, the free two Br ions occupied the counter ion position far away from each other yielding mixed dication $[Cu(phen)(triene)]Br_2$ complex. The 5-fold coordinated Cu^{2+} ion is in a highly distorted square pyramidal environment, the trans angles of the square base are 175.09(16)° and 155.92(15)°, the average angles between the axial atom N10, Cu1 and the equatorial atoms (base atoms; N1, N3, N4 and N5) is 97.0° (range = 78.85(16)° – 109.66(14)°). The axial bond distance (Cu1-N10) is 2.212(4) Å. The structural features of the desired complex in this work are very similar to $[Cu(dien)(phen)](ClO_4)_2$ reported one [46-51], with one of the two N atoms of phen occupying the apical site Cu-N(apical) bond distance = 2.186 Å, and the other basal site Cu-N(basal) bond distance = 2.022 Å. The disposition of the uncoordinated phen is basically parallel to the Cu bonded phen with dihedral angle between the planes of both of 2.40° as is shown in Fig.2. The uncoordinated phen is linked to the coordinated complex *via* N-

H…N H-bonding connections. The N-H…N bifurcated H-bonding connections parameters are listed in Table 3 (Fig. 3).

The three water molecules in the hydrated complex are hydrogen bonded to the two Br^- ions in the asymmetric unit as is shown in Fig. 3. The water O and Br^- distances vary in distance between 3.386 and 3.639Å. The N-H…N interactions connect the cationic complex and the free phen ligand to a chain structure in run *[101]* direction.

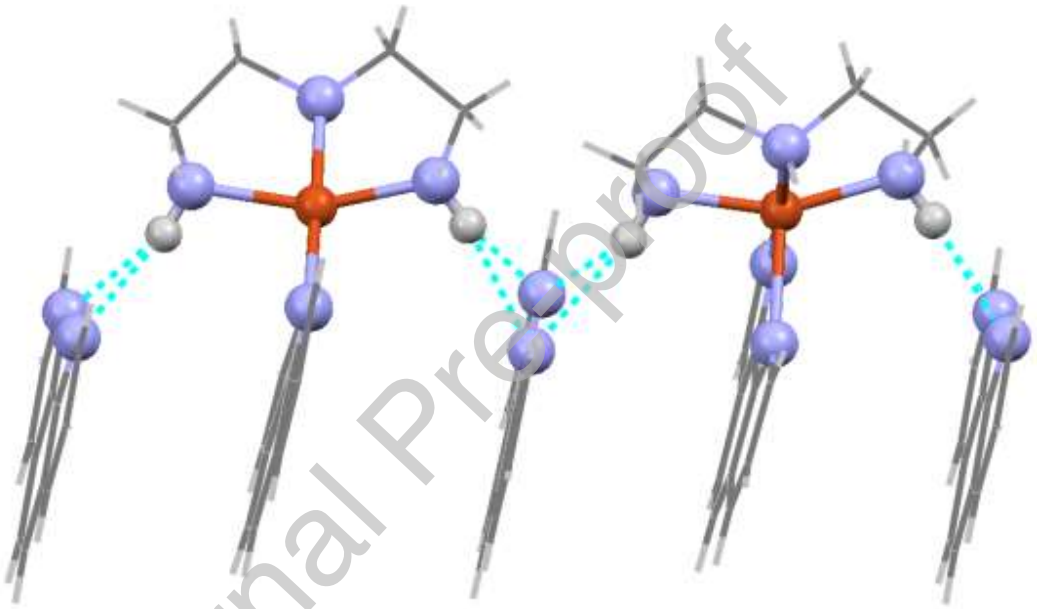

Fig. 3. Chain structure of **1**. All atoms are represented as wireframes except nitrogen atoms that are implicated in the interactions as spheres.

Table 3. Hydrogen bonds distances (Å) and angles (°).

D-H	A	d(H..A)	d(D..A)	<DHA>
N5-H5'A	N19	2.35	3.163(6)	152.3
N5-H5'A	N28	2.56	3.287(6)	140.0

N5-H5'B	O1[a]	2.11	2.953(8)	157.3
N3-H3'A	Br2	2.72	3.468(4)	142.3
N3-H3'B	N19[b]	2.47	3.266(6)	149.1
N3-H3'B	N28[b]	2.53	3.242(6)	137.6
N4-H4'A	Br1	2.55	3.497(4)	161.3

[a][-x+3/2, y+1/2, -z+1/2], [b] x-1/2, -y+1/2, z-1/2

3.4. UV-Vis. and TD-DFT

At room temperature, the complexes absorptions were recorded experimentally in water then assigned with the TD-DFT method. The spectra of the two complexes exhibit intense signals ($\varepsilon = 1.6\times10^{3}$ M^{-1} cm^{-1}) around 280 nm along with a low intensity band around 610 nm ($\varepsilon = 3.5\times10^{2}$ M^{-1} cm^{-1}). For better understanding the electronic structures, DFT stimulations have been carried out for **1** and **2**. The full geometry optimizations for the compounds have been performed at the DFT/UB3LYP level. Some elected optimized bond parameters for **1** are listed in Table 4. The optimized structure parameters of the bond lengths and angles correlated well with the XRD-data of **1**. Contour plots of selected molecular orbitals are shown in Fig. 4.

α-spin molecular orbital		
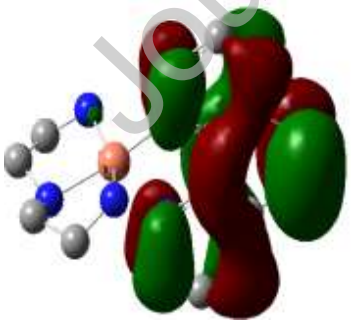	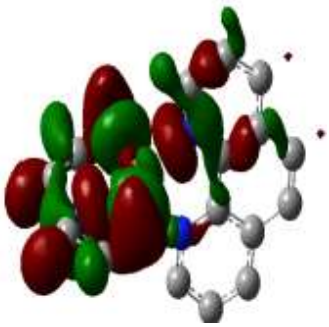	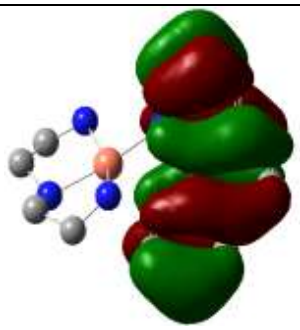
HOMO	HOMO-1	HOMO-2

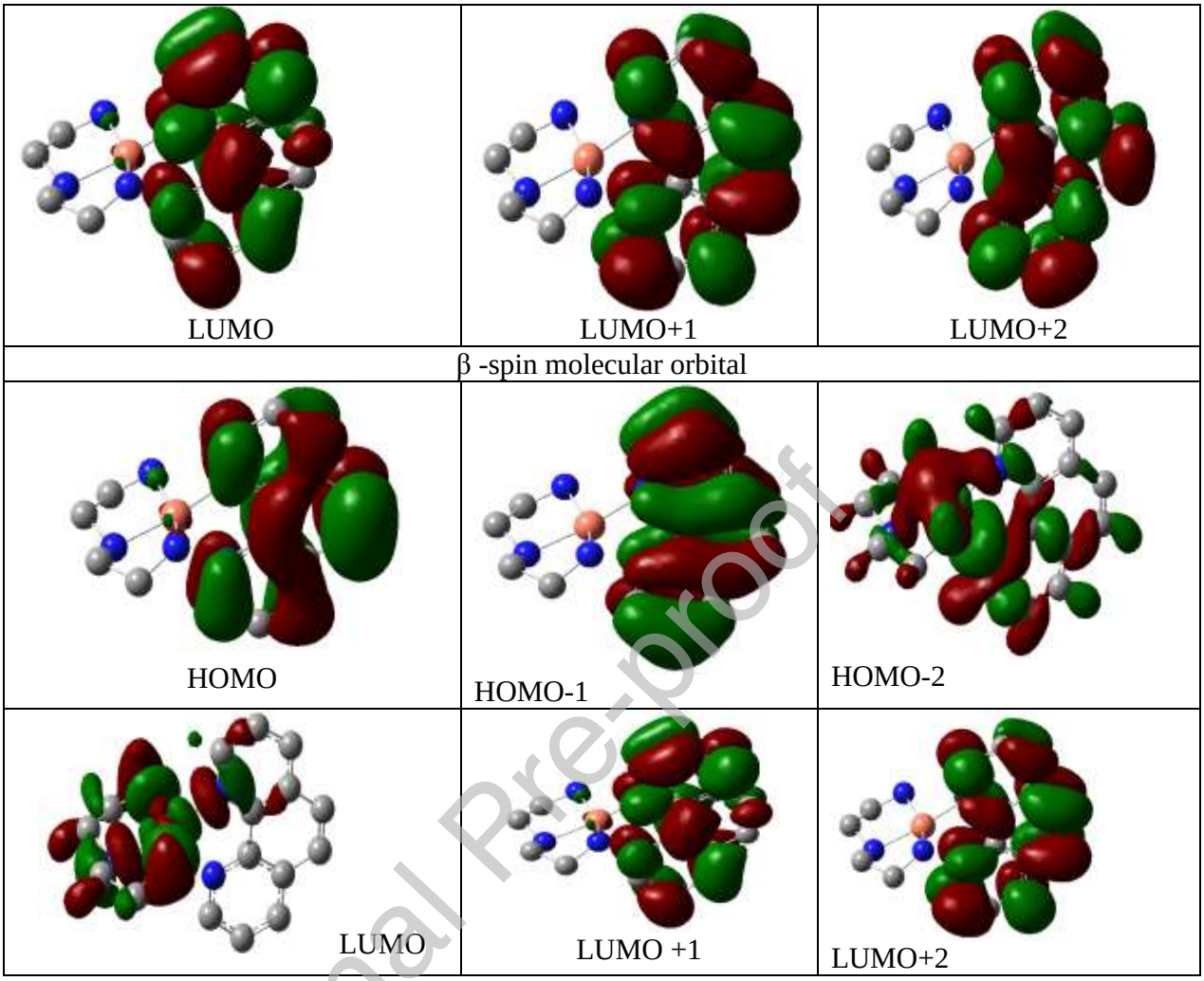

Fig. 4. Isodensity plots of some selected MOs (α-spin and β -spin) of **1**.

Computation of 20 excited states of **1** and **2** allowed the interpretation of the experimental spectra in the range of 200–800 nm (Fig. 5). The calculated energy of excitation states and transition oscillator strength (*f*) are shown in Table 4. Based on the TD-DFT obtained results, both the exp. UV–Vis and the corresponding DFT simulated spectra result are in satisfactory agreement (Fig. 5). In **1**, the two observed absorption bands are due mainly to the transitions from different orbitals to LUMO-α and LUMO-β. The longer wavelength is a result of transition

to LUMO-β that is mainly composed mainly from Cu (58%) and triamine ligand (33%). The shorter wavelength is due to the transition to LUMO-α which is mainly located on phen.

Table 4. DFT energies and composition of selected highest occupied (H) and lowest unoccupied (L) molecular orbitals of both complexes expressed in terms of composing fragments.

Complex **1**									
α MO					β MO				
MO	eV	phen	Cu	Triemine	MO	eV	phen	Cu	triemine
L+4	-0.03	2	80	17	L+3	-1.18	99	1	1
L+3	-0.43	99	1	0	L+2	-2.34	100	0	0
L+2	-1.18	99	1	0	L+1	-2.53	98	1	0
L+1	-2.33	100	0	0	L	-3.88	9	58	33
L	-2.56	98	1	0	H	-7.12	99	0	1
H	-7.13	99	0	0	H-1	-7.52	100	0	0
H-1	-7.51	18	19	64	H-4	-8.79	30	11	59
H-2	-7.53	100	0	0	H-7	-9.77	59	31	10
H-3	-8.13	67	23	11	H-9	-10.04	64	20	17
H-4	-8.92	57	6	36	H-10	-10.16	30	48	22
H-7	-9.14	43	7	49	H-11	-10.24	15	68	16
Complex **2**									
α MO					β MO				
MO	eV	phen	Cu	Triemine	MO	eV	phen	Cu	triemine
L+5	0.02	1	90	9	L+5	-0.14	1	77	22
L+4	-0.16	1	76	23	L+4	-0.43	99	1	1
L+3	-0.43	99	1	1	L+3	-1.17	98	1	1
L+2	-1.17	98	1	1	L+2	-2.33	100	0	0
L+1	-2.33	100	0	0	L+1	-2.52	99	1	1
LUMO	-2.54	99	1	0	LUMO	-3.85	9	57	34
HOMO	-7.12	99	0	0	HOMO	-7.12	99	0	1
H-1	-7.33	14	17	69	H-1	-7.52	100	0	0
H-2	-7.52	100	0	0	H-2	-7.88	59	30	11
H-3	-8.09	69	22	9	H-3	-8.52	24	11	65
H-4	-8.87	32	6	62	H-4	-8.66	10	10	81

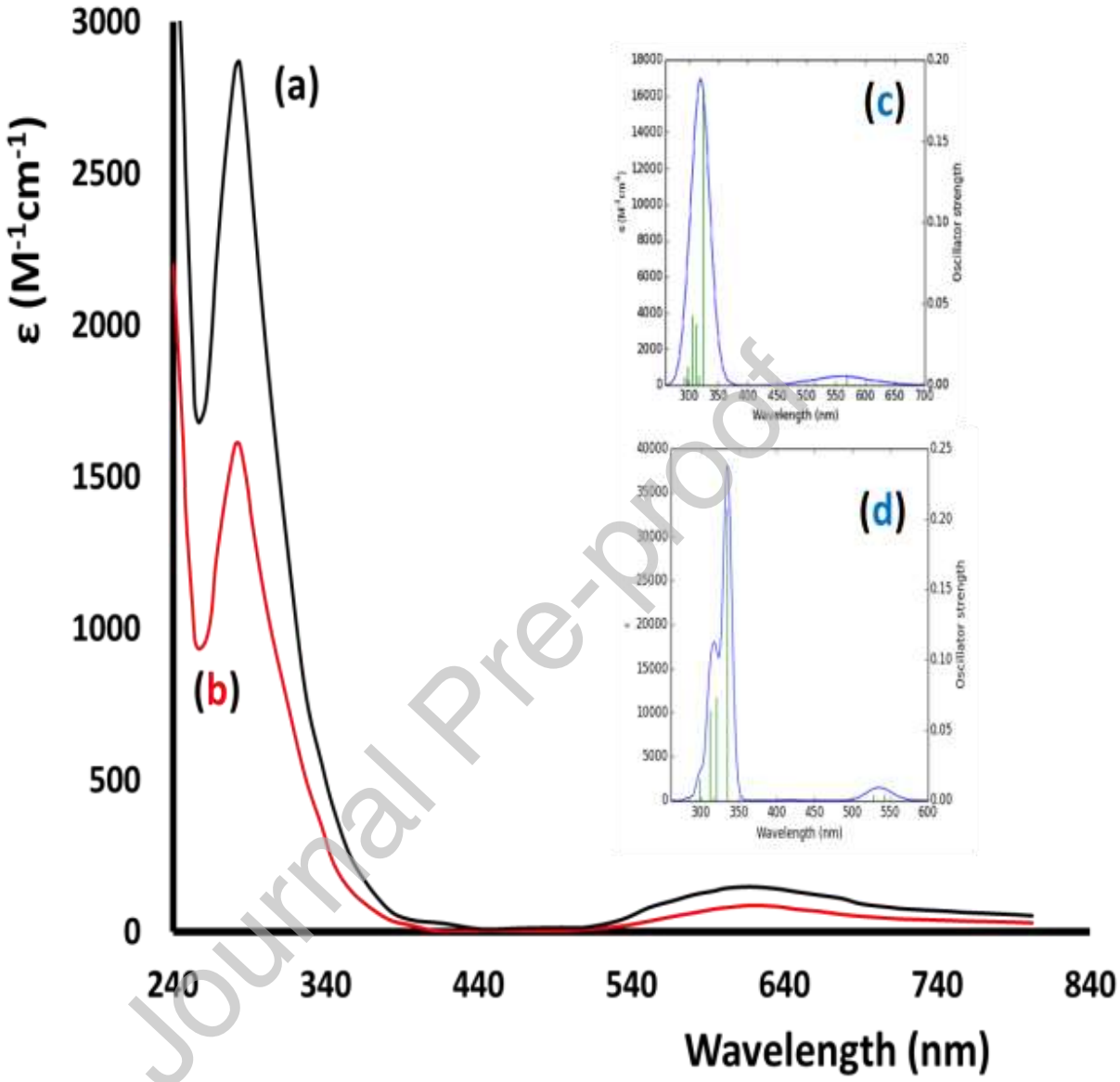

Fig.5. RT UV-Vis. spectra, (a) **1**, (b) **2**, and (c) TD-DFT of **1** and (d) **2** in water.

Table 5. Computed excitation energies (nm), electronic transition configurations and oscillator strengths (*f*) for the optical transitions in the visible region of both complexes transitions with $f \geq$ 0.001 are listed).

For Complex **1**		
λ (nm)	f	Composition
568.9	0.0057	H-16(β) →LUMO (β) (12%), H-10(β) →LUMO (β) (18%), H-9(β) →LUMO (β) (15%), H-3(β) →LUMO (β) (27%), HOMO (β) →LUMO (β) (18%)
512.7	0.0022	H-13(β) →LUMO (β) (18%), H-11(β) →LUMO (β) (53%), H-7(β) →LUMO (β) (12%)
323.9	0.1822	H-4(β) →LUMO (β) (72%)
316.4	0.0058	HOMO (α) →LUMO (α) (35%), H-4(β) →LUMO (β) (15%), HOMO (β) →L+1(β) (35%)
311.2	0.038	H-1(α) →LUMO (α) (34%), H-3(β) →LUMO (β) (34%)
304.9	0.0431	H-1(α) →LUMO (α) (36%), H-3(β) →LUMO (β) (23%)
298.5	0.0119	H-2(α) →LUMO (α) (18%), HOMO (α) →L+1(α) (30%), H-1(β) →L+1(β) (19%), HOMO (β) →L+2(β) (29%)
For Complex **2**		
λ (nm)	f	Composition
542.5	0.0046	H-14(β) →LUMO (β) (36%), H-10(β) →LUMO (β) (25%),
528.2	0.0045	H-13(β) →LUMO (β) (19%), H-11(β) →LUMO (β) (29%)
335.0	0.2081	H-3(β) → LUMO (β) (81%)
320.3	0.0732	H-1(β) → LUMO (α) (31%), H-4(β) → LUMO (β) (50%)
316.5	0.0025	HOMO (A) → LUMO (A) (39%), HOMO (B) → L+1(B) (40%)
311.6	0.0645	H-1(α) →LUMO (β) (56%), H-4(β) → LUMO (β) (28%)
298.5	0.0157	H-2(α) → LUMO (α) (18%), HOMO (α) → L+1 (α) (30%), H-1(β) → L+1(β) (18%), HOMO (β) → L+2(β) (30%)

On the basis of its intensity and position, the high intensity and energy band at 282 nm result from the overlap of two calculated transitions 311 nm resulted from the overlap of three transitions 304.9 nm which is resulted from H-1(α) to LUMO (α) and H-3(β) to LUMO (β), 311.2 nm resulted from H-1 to L (α) and H-3(β) to LUMO (β) (34%) and 323.9 nm which is resulted from H-4(β) →LUMO (β) (Table 5) thus this band is assigned as to Phen(π)→Phen(π*) transitions. The low intensity lowest energy band at 610 nm resulted from the overlap of two calculated transition (512.7 m which is resulted from HOMO/-3 /-9/-10/-16(β) to L (β) and 512.7 nm resulted from H-7/ -11/-13(β) to L(β)) thus, this band is a assigned to a of d–d transition of Cu(II) ions which is typical for a distorted trigonal bipyramidal coordination geometry around copper(II) [22].

3.5. Global reactivity descriptor (GRD)

The GRD quantum parameters such as ionization potential (I), electron affinity (A), electronegativity (χ), hardness (η), chemical potential (μ), softness (σ), and electrophilicity (ω) of **1** and **2** were calculated using the following equations then listed in Table 6.

I: *Ionization potential* $= -E_{HOMO}$ (1)
A: *Electron affinity* $= -E_{LUMO}$ (2)
ΔE_{gap}: *Energy gap* $= E_{HOMO} - E_{LUMO}$ (3)
χ: *Absolute electronegativity* $= (I + A)/2$ (4)
η: *Global hardness* $= (I - A)/2$ (5)
σ: *Global softness* $= l/2\eta$ (6)
μ: *Chemical potential* $= -\chi$ (7)
ω: *Electrophilicity* $= \mu^2/2\eta$ (8)

Table 6. GRD values for both complexes.

GRD		**1**	**2**
Low unoccupied molecular orbital	LUMO	-0.10282 a.u.	-0.10451 a.u
High occupied molecular orbital	HOMO	-0.14042 a.u.	-0.13053 a.u.
Energy gap	ΔE_{gap}	0.0376 a.u.	0.0261 a.u.
		1.0232 eV	0.7101 eV
Ionization potential	I	3.8210 eV	3.5520 eV
Electron affinity	A	2.7979 eV	2.8439 eV
Absolute electronegativity	X	3.3005 eV	3.1979 eV
Global hardness	η	0.5115 eV	0.35405 eV
Global softness	Σ	0.9775 eV	1.4145 eV
Chemical potential	M	-3.3005 eV	-3.1979 eV

Electrophilicity	ω	10.645 eV	14.6282 eV

As can be seen from Table 6, the GRD quantum parameters of both complexes are much closed in their values, such seen is not surprising since the different in both structures of the complexes is very small.

3.6. Solvatochromism

The Cu(II) complexes with d^9 expected to have strong John-Teller effect that permit the performance of further solvatochromic studies [22-29]. The desired complexes were found to have low solubility in organic solvents; therefore, the number of solvents introduced in this study was limited to five. The type of solvent resulted in the observation of different values for λ_{max} in both complexes, for instance, acetonitrile showed λ_{max} at 585 nm, methyl acetate at 600 nm, water at 610 nm, DMF at 625 nm, and DMSO at 640 nm for complex **1** as illustrated in Fig.6a. For complex **2** acetonitrile showed λ_{max} at 560 nm, methyl acetate at 602 nm, water at 610 nm, DMF at 647 nm, and DMSO at 680 nm as illustrated in Fig.6b. In order to learn more about the solvatochromism behavior of the desired complexes, Gutmann's relations have been established. No clear regular relation was observed by plotting AN solvents numbers versus the changes in λ_{max} values (Fig.6c for **1** and Fig.6d for **2**). Meanwhile plotting DN solvents values against λ_{max} values, resulted in a linear appositive relationship with a correlation factor $R^2 = 0.9412$ as seen in Fig.6e for **1** and $R^2 = 0.9495$ as seen in Fig.6f for **2**. It is evident that, both complexes have similar solvatochromism behavior the d-d bands were shifted with increasing solvents DN values with bathochromic pattern (red shift), therefore, the complexes are expected to have a Lewis acid behaviors.

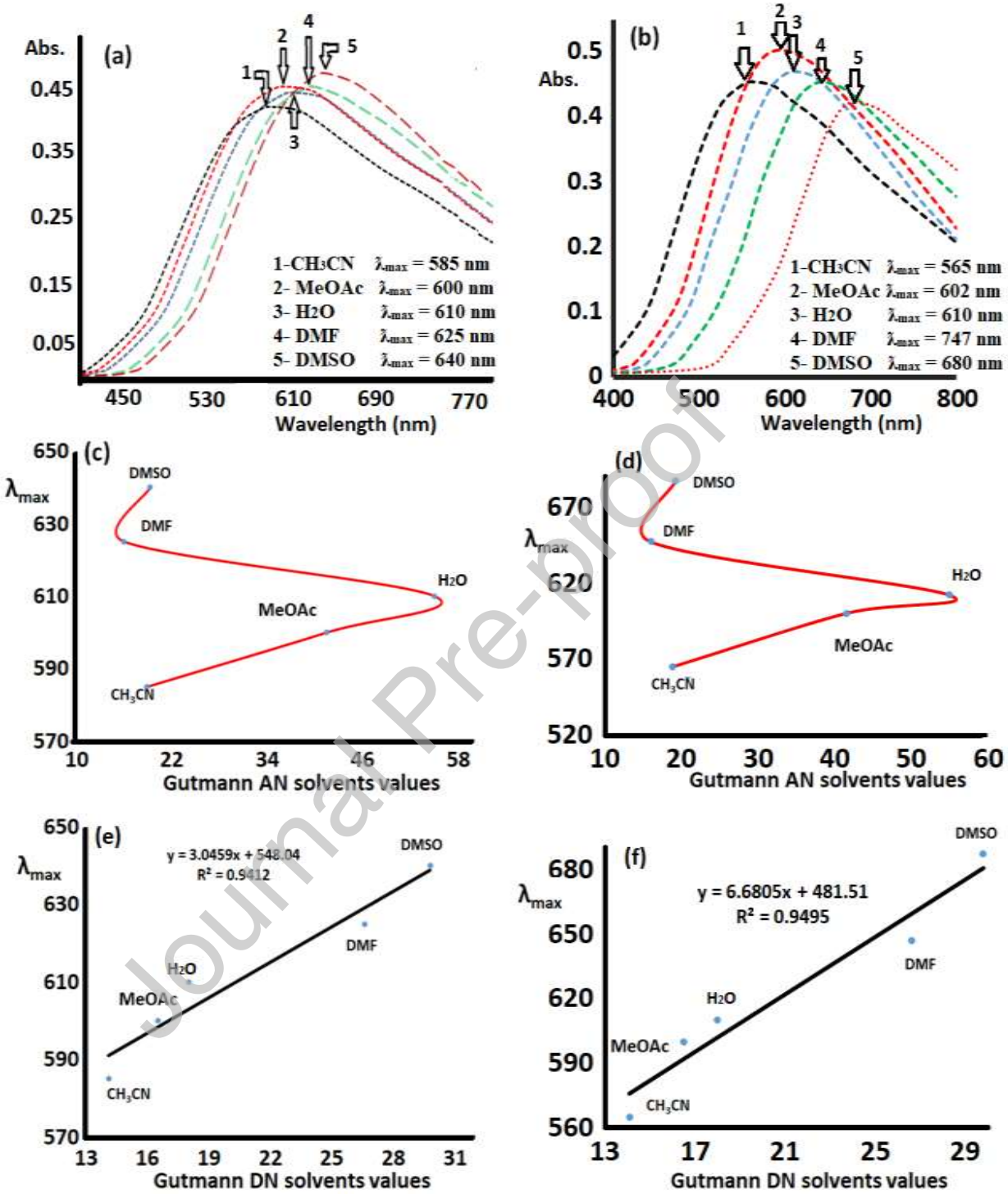

Fig.6. Solvatochromism spectra: (a) Abs. vs. λ_{max} for **1**, (b) Abs. vs. λ_{max} for **2**, (c) AN vs. λ_{max} for **1**, (d) AN vs. λ_{max} for **2**, (e) DN vs. λ_{max} for **1**, and (f) DN vs. λ_{max} for **2**.

3.7. TGA investigation

The TGA behavior of **1** was investigated as seen in Fig.7. The TG/DTA curves were performed in a temperature range of 0–900 ^{o}C and at 5 ^{o}C/min heating rate under RT atmosphere. The TGA analyses of **1** reflected a process of degradation occurring in 3 consecutive steps: dehydration, de-structuring of the N-ligands and metal-oxide formation. The dehydration of the uncoordinated water molecule was the first step recorded at 95-120 ^{o}C with T_{DTA} at 110 ^{o}C (endothermic sign) and 8% mass lost. The de-structuring of the phen and triamine ligands was the second step occurred in 180-480 ^{o}C range with 40% mass lost and T_{DTA} at 250 and 480 ^{0}C (both exothermic), moreover, this step ended by naked $CuBr_2$ complex formation. Oxidation of $CuBr_2$ complex to Cu=O with 23% mass occurred in range of 500 to 710 ^{o}C temperature with exothermic step at T_{DTA} = 680 ^{o}C. The Cu=O copper oxide final product was supported by IR analysis [22-28].

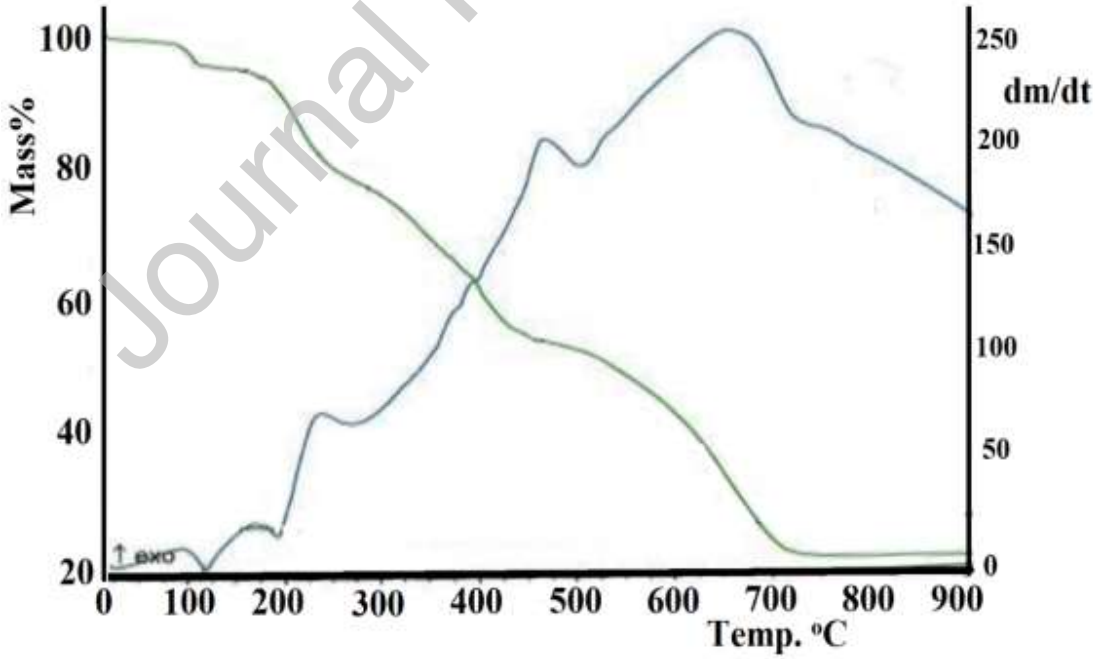

Fig.7. TGA of **1.**

3.8. DNA binding properties of 1: Electronic spectral

The electronic absorption spectroscopy was used to study possibility of the complex-DNA binding [52-55]. The complexes readiness to bind the DNA usually results in bathochromism and hypochromism which depend on the nature of the intercalative interactions including ring stacking between the base pairs of the DNA and the aromatic rings in complexes. The extension of the hypochromism usually reflected the presence of the intercalative binding. The absorption of $5x10^{-3}$ M of **1** in Tris–HCl buffer revealed bands at 620 and 280 nm. At the visible 610 nm absorption band CT-DNA titration was performed as seen in Fig.8I. Upon incremental addition of $1.00x10^{-5}$ –0.04 M DNA, the band shows sufficient decay in absorption accompanied (Fig.8II).

In order to compare quantitatively the strength of binding of the desired complexes, the calculated K_b intrinsic binding constant was determined by controlling the changes in absorbance with increasing concentration of DNA using the following equation: [22, 23].

$$[DNA]/(\varepsilon_a - \varepsilon_f) = [DNA]/(\varepsilon_b - \varepsilon_f) + 1/(Kb\ (\varepsilon_b - \varepsilon_f)$$

Wherein [DNA] is the concentration of DNA in base pairs, ε_a, ε_f, and ε_b are the apparent-, free- and bound-metal-complex extinction coefficients respectively. Kb is the equilibrium-binding constant (in M^{-1}) of complex binding to DNA. When plotting $[DNA]/(\varepsilon_a-\varepsilon_f)$ *vs* [DNA], K_b is obtained by the ratio of the slope to the intercept.

The K_b for **1** is found to be 4.6 x 10^4 M^{-1} (Fig.8III), whereas **2** showed similar DNA binding behavior with slightly less K_b value ($4.1x10^4$ M^{-1}). These results are comparable to those previously recorded for similar Cu(II) complexes [51]. The results suggested a strong

intercalation of such complexes with double helix of the DNA as cis-plat mode of coordination [51-54].

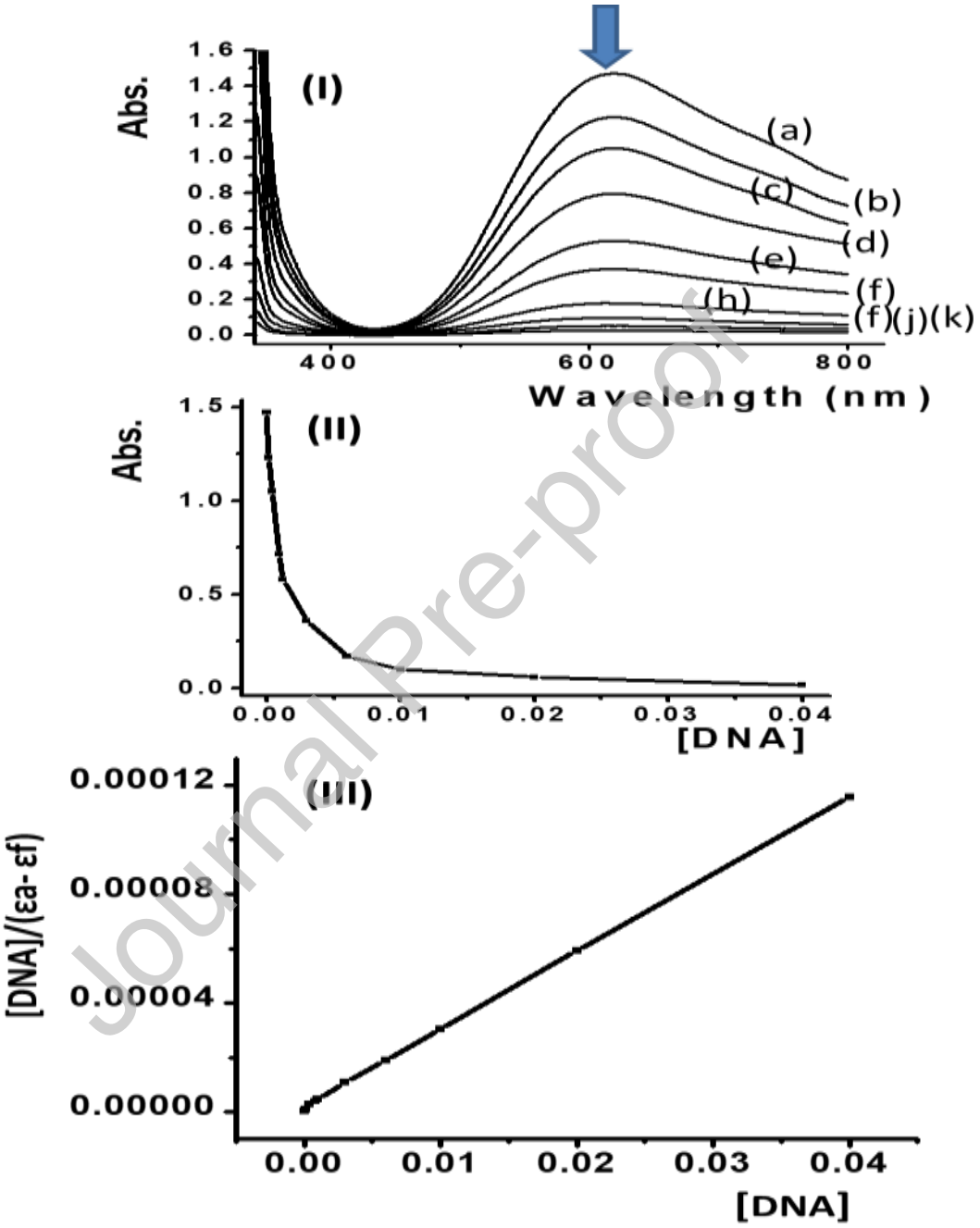

Fig. 8. a) Electronic spectral titration of **1** with CT-DNA at 620 nm in Tris-HCl buffer; [**1**] = 5 × 10^{-3}; [DNA]: (*a)* 0.0, (*b)* 1.0 × 10^{-4}, (*c)* 4.0 × 10^{-4}, (*d)* 8.0 × 10^{-4}, (*e)* 1.0 × 10^{-3}, (*f)* 3.0 × 10^{-3},

(*h)* 6.0 × 10^{-3}, (*i)* 1.0 × 10^{-2}, (*j*) 2.0 × 10^{-2} , (*k*) 4.0 × 10^{-2} M. The arrow denotes the gradual decrease of the complex concentration upon DNA addition. b) Absorption plot against [DNA] to confirm the exponential decreasing relation at 620 nm. c) Plot of [DNA]/(ε_a- ε_f) *vs.* [DNA] for the absorption titration of DNA with the **1**.

4. Conclusions

Two dicationic mixed-ligand triamine/1,10-phenanthroline/Copper(II) complexes were synthesized in excellent yields under ultrasonic mode of vibration. The disconnection of 2Br from $CuBr_2$(phen) by dien or dipn N-tridentate ligand from the internal coordination sphere to the outer sphere was monitored by UV-visible, IR, and confirmed by XRD. The XRD results for **1** showed that Cu(II) center is coordinated to 5 N-donor (phen and triamine) ligands with two Br counter ions salt in a highly distorted square pyramidal shape. The self-assembly of **1** indicated that the N(π)…N interactions play a considerable part in stabilizing the final three-dimensional structure. The absorption behaviors of the prepared complexes in water were modeled by TD-DFT. The solvatochromism showed positive Gutmann's relationship with several DN solvents. The desired complexes exhibited a strong DNA binding; the absorption spectral K_b constant values are in similar complexes ranges.

Conflicts of interest

The authors declare that they have no conflicts of interest.

Acknowledgement

Researchers Supporting Project number (RSP-2020/160), King Saud University, Riyadh, Saudi Arabia.

References

1. S. Chandra, L.K. Gupta, Sangeetika. Spectrochim. Acta, Part A, 62, (2005) 453-460.
2. K.P. Balasubramanian, K. Parameswari, V. Chinnusamy, R. Prabhakaran, K. Natarajan. Spectrochim. Acta, Part A, 65 (2006) 678-683.
3. K.P. Balasubramanian, R. Karvembu, R. Prabhakaran, V. Chinnusamy, K. Natarajan. Spectrochim. Acta, Part A, 68 (2007) 50-54.
4. T. Rosu, E. Pahontu, C. Maxim, R. Georgescu, N. Stanica, A. Gulea. Polyhedron 30 (2011) 154-162.
5. P. Sathyadevi, P. Krishnamoorthy, M. Alagesan, K. Thanigaimani, P. Thomas Muthiah, N. Dharmaraj. Polyhedron, 31 (2012) 294-306.

6. K.M. Vyas, R.G. Joshi, R.N. Jadeja, C.R. Prabha, V.K. Gupta. Spectrochim. Acta, Part A, 84 (2011) 256-268.
7. R. Karvembu, S. Hemalatha, R. Prabhakaran, K. Natarajan. Inorg. Chem. Commun., 6, (2003) 486-490.
8. G.D. Frey, Z.R. Bell, J.C. Jeffery, M.D. Ward. Polyhedron, 20 (2001) 3231-3237.
9. F. Mevellec, S. Collet, D. Deniand, A. Reliquet, J.C. Meslin. J. Chem. Soc., Perkin Trans. 1 (2001) 3128-3131.
10. D. S. Sigman, A. Mazumder, D. M. Perrin, Chem. Rev. 93 (1993) 2295- 2316.
11. A. Sigel, H. Sigel (Eds.), Metal Ions in Biological Systems Proving of Nucleic Acids by Metal Ion Complexes of Small Molecules, vol. Marcel Dekker, New York, 1996.
12. D. R. McMillin, K. M. McNett Chem. Rev. 98 (1998) 1201-1220.
13. K.E. Erkkila, D.T. Odom, J.K. Barton, Chem. Rev. (1999) 2777-2796.
14. J. Leiter, J.L. Hartwell, J.S. Kahler, I. Kline, M.J. Shear, J. Natl. Cancer Inst. 14 (1963) 365-409.
15. C. Krishnamurty, L.A. Byran, D.H. Petering, Cancer Res. 40 (1980) 4092-4099.
16. R.J. Sorenson, Chem. Br. 16 (1984) 1110‑1113.
17. P. Kopf-Maier, H. Kopf, Chem. Rev. 87 (1987) 1137‑1152.
18. S.E. Scherman, S.J. Lippard, Chem. Rev. 87 (1987) 1153‑1181.
19. M.J. Chare, P.C. Hydes, in: H. Sigel (Ed.), Metal Ion in Biological Systems, vol. 2, Marcel Dekker, New York, 1980, pp. 1–62.
20. K. Takamiya, Nature (London) 185 (1960) 190-191.
21. M. Al-Noaimi, A. Nafad, I. Warad, R. Alshwafy, A. Husein, W. H. Talib, T. Ben Hadda Spectrochimica Acta Part A: Molecular and Biomolecular Spectroscopy 122 (2014) 273‑282.
22. M. Al-Noaimi, M. I. Choudhar, F. F. Awwadi, W. H. Talib,T. Ben Hadda, S. Yousuf, A. Sawafta, I. Warad, Spectrochimica Acta Part A: Molecular and Biomolecular Spectroscopy 127 (2014) 225–230.
23. K. Hema, I. Warad, S. Karthik, A. Zarrouk, K. Kumara, J. Pampa, P. Mallu, K. Lokanath, J Mol Struct 1210 (2020) 128000-128010.
24. I. Warad, F. F. Awwadi, B. Abd Al-Ghani, A Sawafta, N. Shivalingegowda, N. K. Lokanath, M.S. Mubarak, T. Ben Hadda, A. Zarrouk, F. Al-Rimawi, A. B. Odeh, S. A. Barghouthi, Ultrasonics Sonochem. 48 (2018) 1-14
25. I. Warad, S. Musameh, A. Sawafta, P. Brandão, C. J. Tavares, A. Zarrouk, S. Amereih, A. Al Ali, R. Shariah. Ultrasonics Sonochem. 52 (2019) 428-432
26. F. A. Saleemh, S. Musameh, A. Sawafta, P. Brandao, C. J. Tavares, S. Ferdov, A. Barakat, A. Al Ali, M. Al-Noaimi, I. Warad. Arab. J. Chem. 10 (2017) 845-855.
27. N. Al-Zaqri, K.S.M. Salih, F.F. Awwadi, A. Alsalme, F.A. Alharthi, A. Alsyahi, A. Al Ali, A. Zarrouk, M. Aljohani, A. Chetouni, I. Warad, J. Coord. Chem. 73 (2020) 3236–3248
28. M.K. Hema, C.S. Karthik, N.K. Lokanath, P. Mallu, A. Zarrouk, K.S.M. Salih, I. Warad, J. Mol. Liq. 315 (2020) 113756-113762.
29. T. Hadda, A. Ali, V. Masand, S. Gharby, T. Fergoug, I. Warad, Med. Chem. Res., 22 (2013) 1438-1449.
30. M. El Faydy, F. Benhiba, B. Lakhrissi, M. Ebn Touhami, I. Warad, F. Bentiss, A. Zarrouk, J. Mol. Liq., 295 (2019) 111629-111645.

31. Gaussian 09, Revision A.1, M.J. Frisch, G.W. Trucks, H.B. Schlegel, et. al., Gaussian Inc, Wallingford CT, 2009, Gaussian: Pittsburgh, PA.
32. P.J. Hay, W.R. Wadt, J. Chem. Phys. 82 (1985) 270–283.
33. R. Bauernschmitt, R. Ahlrichs, Chem. Phys. Lett. 256 (1996) 454–464.
34. M.K. Casida, C. Jamorski, K.C. Casida, D.R. Salahub, J. Chem. Phys. 108 (1998) 4439–4449.
35. R. E. Stratmann, G.E. Scuseria, M.J. Frisch, J. Chem. Phys. 109 (1998) 8218–8224.
36. M. Cossi, N. Rega, G. Scalmani, V. Barone, Comput. Chem. 24 (2003) 669–681.
37. CrysAlisPro, Agilent Technologies, Version 1.171.35.11 (release 16-05-2011 CrysAlis171 .NET) (compiled May 16 2011).
38. Sheldrick G. M. SHELXTL version 6.10 (2000) Structure determination software suite. Bruker AXS Inc., Madison, WI.
39. G.A. Gazzani, A. Papetti, G. Massolini, M. Daglia. J. Agric. Food Chem. 46 (1998) 4118- 4122.
40. S. Destri, M. Pasini, W. Porzio, F. Rizzo, G. Dellepiane, M. Ottonelli, G. Musso, F. Meinardi, L. Veltri, J. Lumin. 127 (2007) 601-605.
41. P. Vijayan, P. Vijayaraj, P. Setty, C. Hariharpura, A. Godavarthi, S. Badami, D.Arumugam, S. Bhojraj Biol Pharm Bull. 24 (2004) 528–530.
42. C. Tsiamis, M. Themeli, Inorg. Chim. Acta 206 (1993)105-115.
43. K. Nakamoto, Infrared and Raman spectra of Inorganic and Coordination Compounds, 4th ed.; J. Wiley & Sons: NY, 1986.
44. A. Cassol, P. Di Bernardo, R. Portanova, M. Tolazzi, G. Tomat, P. Zanonato, J. Chem. Soc., Dalton Trans. (1992) 469-474.
45. R. N. Patel, N. Singh, K. Shukla, J. Niclos-Gutierrez, A. astineiras, V. G. Vaidyanathan, B. Unni Nair, Spectrochimica Acta Part A 62 (2005) 261–268.
46. N. Al-Zaqri, K.S.M. Salih, F.F. Awwadi, A. Alsalme, F.A. Alharthi, A. Alsyahi, A. Al Ali, A. Zarrouk, M. Aljohani, A. Chetouni, I. Warad, J. Coord. Chem. *73* (2020) 3236-3248.
47. R.N. Patela, N. Singha, K.K. Shuklaa, J. Niclos-Gutierrez, A. Castineirasb, V.G. Vaidyanathanc, B. U. Nairc, Spectrochimica Acta Part A 62 (2005) 261–268.
48. G. Andara, F. Fortes-Revilla, C. Snejko, N. Gutierrez-Puebla, E. Iglesias, M. Monge, M. A. Inorg. Chem. 45 (2006) 9680–968
49. F. F. Awwadi, D. Willett, D. Twamley, Cryst. Growth Des., 7 (2007) 624-632.
50. F. F. Awwadi, D. Willett, K. Peterson, B. Twamley, J. Phys. Chem. A, 111 (2007) 2319-2328.
51. E. Lindner, S. Al-Gharabli, I. Warad, H. A. Mayer, S. Steinbrecher, E. Plies, M. Seiler, H. Bertagnolli, Anorg. Allg. Chem. 629 (2003) 161-171

52. I. Warad, H. Suboh, N. Al-Zaqri, A. Alsalme, F. A. Alharthi, M. M. Aljohani, A. Zarrouk, RSC Adv. 10 (2020) 21806–21821.
53. S. K. Maiti, M. Kalita, A. Singh, J. Deka and P. Barman, Polyhedron, 184 (2020) 114559–114566.
54. Z. Afsan, T. Roisnel, S. Tabassum and F. Arjmand, Bioorg. Chem., 94 (2020)103427–103438.
55. R. Kalarani, M. Sankarganesh, G. G. V. Kumar and M. Kalanithi, J. Mol. Struct., 2020, 127725–127732.

Graphical Abstract